HYDROGEN-PLASTICITY INTERACTIONS NEAR A CRACK TIP: A FRACTOGRAPHIC AND NUMERICAL STUDY

J. Toribio and V. Kharin
Department of Materials Engineering, University of Salamanca
E.P.S., Campus Viriato, Avda. Requejo 33, 49022 Zamora
Tel: 980 545 000; Fax: 980 545 002, E-mail: toribio@usal.es

Abstract. This paper deals with the effects of plasticity generated in the vicinity of a crack tip by previous cyclic (fatigue) loading and posterior monotonic loading on hydrogen assisted cracking (HAC). Experiments are considered in combination with a high-resolution numerical modelling of the elastoplastic stress-strain field near the crack tip, so that the plastic zone extent is compared with the size of the hydrogen-assisted micro-damage region or *tearing topography surface* (TTS). In most of the analysed cases the TTS region clearly exceeds the plastic zone and does not have any relation with it, i.e., the hydrogen affected area exceeds the only region in which there is dislocation movement, and the hydrogen transport cannot be attributed to dislocation dragging, but only to diffusion. It is, however, stress assisted diffusion in which the hydrostatic stress field plays a relevant role.

Resumen. Este artículo trata de los efectos de la plasticidad generada en las proximidades del extremo de una fisura mediante solicitación previa oscilante (fatiga) y solicitación posterior monótona creciente en condiciones de fisuración asistida por hidrógeno (FAH). Se analizan los resultados experimentales en conjunción con una modelización numérica de alta resolución del campo tenso-deformacional elastoplástico cerca del extremo de la fisura, de modo que la extensión de la zona plástica se compara con el tamaño de la zona de micro-daño asistido por hidrógeno o *tearing topography surface* (TTS). En la mayoría de los casos analizados la zona TTS sobrepasa claramente la zona plástica y no tiene relación alguna con ella, es decir, la zona afectada por el hidrógeno sobrepasa la única región en la cual hay movimiento de dislocaciones, de modo que el transporte de hidrógeno no puede se atribuido al arrastre dislocacional, sino únicamente a la difusión. Sin embargo, se trata de difusión asistida por la tensión, según la cual el campo de tensión hidrostática juega un papel relevante.

1. INTRODUCTION

The study of hydrogen-plasticity interactions is a fundamental issue to clarify the micromechanisms leading to hydrogen-assisted fracture of metallic materials. The relationship between hydrogen and plasticity has been frequently the object of controversy about two key topics: (i) whether hydrogen influences plasticity by promoting strain localization and (ii) whether or not plastic zone spreading —and corresponding movement of dislocations— can affect hydrogen transport.

Since there is general agreement that hydrogen transport plays a dominant role in hydrogen-assisted cracking (HAC), it is important to elucidate the main hydrogen transport mechanism operative over *relevant* penetration distances. The problem is far from being totally understood, and two main types of hydrogen transport in metals have been proposed: *lattice diffusion* [1-3] (or random-walk diffusion) and *dislocation sweeping* [4-6] (or dislocation dragging).

Diffusion is a transport mode by which hydrogen moves towards the points of minimum concentration, the penetration distance being controlled by the $\sqrt{Dt}$ term [1]. If stress assisted diffusion is considered [2], hydrogen transport is driven by the gradients of concentration and hydrostatic stress. A more general treatment [3] involves also plastic strain gradients contributing to diffusion. A mechanism of hydrogen transport by diffusion is consistent with the results of

slow strain rate tests under cathodic hydrogenation, since it predicts maximum hydrogen effect at the slowest strain rates [7].

Dislocation sweeping is a transport mechanism by which hydrogen is dragged by dislocations as the plastic zone spreads, it being associated with the average velocity of dislocations which may be macroscopically expressed in terms of the plastic strain rate [4]. There are two main models of dislocation sweep-in of hydrogen: the *stripping model* [4] and the *annihilation model* [5], reviewed in [6]. The first predicts a significant build-up of hydrogen, while the latter concludes that the supersaturations of hydrogen are negligible. The weakest point of the two models is their inconsistency with the known experimental evidence of the monotonic inverse dependence of hydrogen embrittlement upon strain rate.

The issue of the controlling hydrogen transport mode was addressed in previous research on hydrogen-assisted fracture in *notched* specimens of high-strength pearlitic steel [8,9], showing that stress-assisted diffusion is the predominant mode of transport in pearlitic steel under triaxial stress states produced by notches and that there is no relationship between the plastic zone extent and the hydrogen-affected region revealed by microscopic examination.

This paper tries to provide more insight into this fundamental question by using precracked samples. Since different fatigue precracking programmes are considered, the effects of prestressing and prestraining in the vicinity of the crack tip are elucidated, which is a very important topic because the fatigue precracking levels affect dramatically the values of stress intensity factor for initiation of HAC [10,11].

2. EXPERIMENTAL PROGRAMME

A high strength eutectoid steel was used, with yield strength σ_Y = 725 MPa, ultimate tensile stress σ_R = 1300 MPa and fracture toughness K_{IC} = 53 MPa $m^{1/2}$. Slow strain rate tests were performed on precracked rods in aqueous solution under electrochemical control, as described elsewhere [12]. The displacement rate was 8.3 x 10^{-8} ms^{-1}, based on experience [13]. A constant electrochemical potential of –1200 mV SCE (cathodic) was held during the tests to promote HAC.

Precracking was carried out by axial fatigue in air environment. Various series of samples were prepared by using different fatigue loads during the last stage of fatigue precracking just previous to the environmentally assisted fracture test so as to control this important experimental variable which clearly influences the results in HAC [12]. The maximum levels of stress intensity factor K during fatigue (the last stage) were $K_{max} = 0.28K_{IC}$, $0.45K_{IC}$, $0.60K_{IC}$ and $0.80K_{IC}$.

Fig. 1 shows the experimental failure load in a hydrogen environment F_{HAC} (divided by the value in air F_C) as a function of K_{max}/ K_{IC}. The effect of fatigue precracking is beneficial for the HAC resistance, since the fracture load in hydrogen is an increasing function of K_{max}. This may be caused by the cyclic plastic zone or the compressive residual stresses near the crack tip after fatigue precracking. The crack tip is prestrained (or prestressed) by fatigue: the higher the cyclic load level, the more pronounced the prestraining/prestressing effect which delays the hydrogen entry and improves material performance in this aggressive environment.

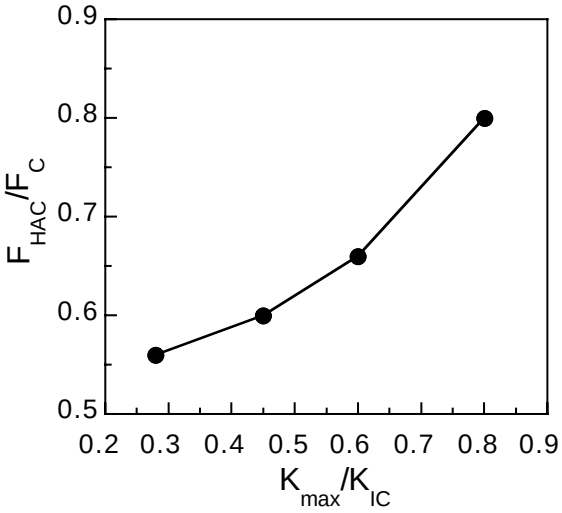

Fig. 1. Ratio of the failure load in hydrogen F_{HAC} to the same in air F_C as a function of the fatigue precracking level expressed by K_{max}/K_{IC}.

The fractographic analysis showed a special fracture mode between the fatigue precrack and the final cleavage fracture: the *tearing topography surface* or TTS [14,15] shown in Fig. 2. This fracture mode is very important in HAC of pearlitic steel because of the experimental evidence which allows its consideration as the hydrogen-assisted micro-damage region, i.e., the zone where the physical micromechanisms of hydrogen-assisted fracture take place [16-18].

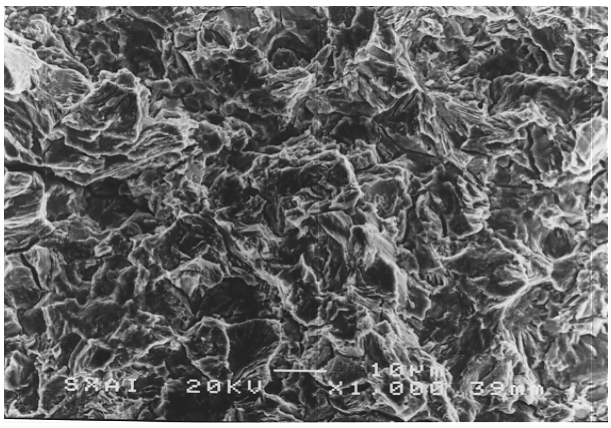

Fig. 2. TTS fracture mode.

The depth of the TTS zone was measured at the deepest point of the crack, in the direction perpendicular to the crack front. Results presented in Fig. 3 show an inverse relationship between the TTS depth and the maximum stress intensity factor level during the last stage of fatigue precracking (K_{max}), i.e., the heavier the fatigue precracking, the narrower the TTS region generated during HAC ahead of the previous fatigue crack front.

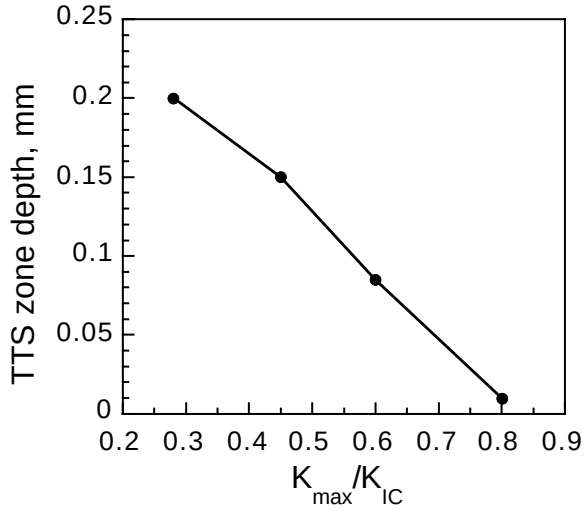

Fig. 3. TTS depth *vs*. K_{max}.

3. NUMERICAL MODELLING

A numerical simulation was made of the stress-strain state near the crack tip under plane-strain small-scale yielding in an elastoplastic material with combined isotropic/kinematic strain-hardening. Its characteristics are those of the steel used in the experiments, cf. [12]. The crack was modelled as a round-tip slit with initial height (twice the tip radius) of 5 μm in agreement with experimental data for fatigue cracks in high-strength steels [19]. The loading history consisted of ten loading cycles in accordance with the experimental fatigue programmes, and rising load corresponding to the HAC test. The nonlinear finite element code MARC [20] was used with updated Lagrangian formulation.

Two crack tip plastic zones are of interest: (i) *forward or monotonic plastic zone*, defined as the domain suffering plastic strain at load maxima ($K=K_{max}$); (ii) *reversed or cyclic plastic zone*, region where plasticity takes place at load minima ($K=K_{min}\cong 0$). The finite element analysis provides the following estimation of the depth of the forward (monotonic) plastic zone at the loading level K_{max}:

$$x_Y = 0.0335\ (K_{max}/\sigma_Y)^2 \qquad (1)$$

The reversed (cyclic) plastic zone at $K_{min}\cong 0$ is also dependent on the previous K_{max}-level (i.e., on the range ΔK). Because of the material's hardening, it is natural to define the plastic flow zone at cyclic loading from the condition of positive increment of the equivalent plastic strain ($d\varepsilon^p_{eq} > 0$). This is the *active*, really cyclic, plastic zone. For cyclic loading under given K_{max}, the depth of this reversed (cyclic) plastic zone at unloading ($K=K_{min}$) may be estimated as:

$$x_\Delta = 0.0065\ (K_{max}/\sigma_Y)^2 \qquad (2)$$

Fig. 4 plots the complete evolution of the depth of the active plastic zone through the whole rising-load HAC process for two different fatigue precracking regimes with $K_{max}/K_{IC} = 0.45$ and 0.80.

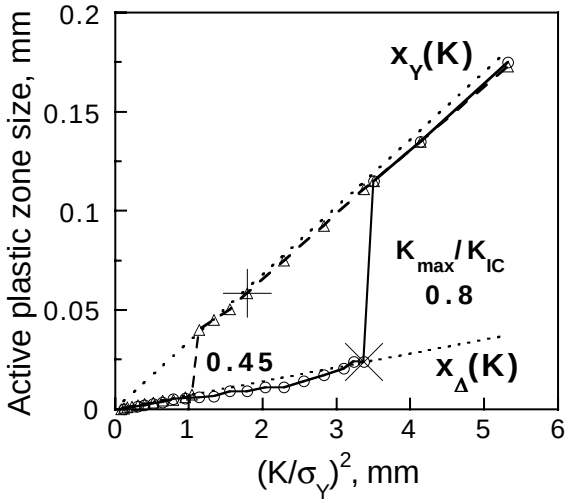

Fig. 4. Evolutions of the depths of active plastic zones in fatigue precracked specimens during rising load HAC tests: dashed and solid lines correspond respectively to fatigue regimes with $K_{max}/K_{IC} = 0.45$ and 0.80, crosses mark the instants of hydrogen assisted fracture in experiments at respective levels of $K = K_{QHAC}$. Points represent the results of the finite element calculations and dotted lines show their approximations by eqs. $x_Y(K) = 0.0335\ (K/\sigma_Y)^2$ and $x_\Delta(K) = 0.0065\ (K/\sigma_Y)^2$.

Fig. 4 allows an analysis of plasticity evolution during the test, as explained in the following paragraphs devoted to sequential phases of the mechanical evolution in the close vicinity of the crack tip:

(i) *Initial phase*. At the beginning of test loading applied after precracking, increasing load causes stresses that, by superposition with the residual stress field after the final load reversal (unloading) in fatigue, result in elastic unloading near the crack tip. Therefore, no plasticity occurs at this phase that lasts up to a certain applied stress intensity factor level slightly dependent on K_{max}. Corresponding average value of the stress intensity factor for initiation of plastic straining in the rising load HAC test for the considered range of K_{max} values may be estimated as $0.2K_{max}$.

(ii) *Intermediate phase*. During further load increase in HAC test, crack tip stress-strain fields evidently evolve

the same way as during previous fatigue load whilst $K \leq K_{max}$, i.e., plasticity development is identical to that observed on the forward portions of load cycles during precracking. So, active plastic deformations detected by the condition $d\varepsilon^p_{eq} > 0$ are confined to the shrunk cyclic plastic zones as described before (path $x_\Delta(K)$ in Fig 4). Neglecting a short interval at the beginning of this phase where for obvious reasons the plastic zone must not be K-controlled and self-similar, relation (2) with K_{max} substituted by applied K turns out to be a good approximation for the plastic zone depth on this stage. Thus the forward active plastic zone in this intermediate phase is $x_\Delta(K) = 0.0065\ (K/\sigma_Y)^2$. The maximum depth attained by the active plasticity in this phase is achieved at $K = K_{max}$ with a value $x_\Delta(K_{max})$.

(iii) *Final phase*. When applied load renders $K > K_{max}$, the equivalence of the stress-defined domain $\sigma_{eq} \geq \sigma_Y$ and the zone of increasing (active) plastic deformation $d\varepsilon^p_{eq} > 0$ is restored since plasticity extends over new portions of material which has not experienced plastic deformation and yields when the initial flow stress σ_Y is attained, so that both of them define the same plastic region. The latter during this stage of the rising load test coincides with the monotonic plastic zone. Then eq. (1) becomes valid again to represent the plastic zone depth. Therefore, when the K value applied during the HAC test exceeds the fatigue precracking level K_{max} the active plastic zone increases in a step-wise manner ("explodes") in this loading stage (path $x_Y(K)$ in Fig. 4).

As a summary, the evolution of the active plastic zone where dislocation motion goes on during the rising load HAC test after fatigue precracking may be described as follows:

$$x_\perp(K) = \begin{cases} 0 & \text{at } K \lesssim 0.2K_{max} \\ x_\Delta(K) = 0.19x_Y(K) & \text{at } 0.2K_{max} \lesssim K \leq K_{max} \\ x_Y(K) & \text{at } K > K_{max} \end{cases} \qquad (3)$$

where the active plastic zone is represented now by the symbol $\perp$ to indicate the material region associated with dislocation movement. For low values of the externally applied K after precracking with K_{max}, i.e., at the beginning of the HAC test ($K \leq 0.2K_{max}$), the active plastic zone is null. Later on ($K \leq 0.2K_{max} < K$), the depth of such a zone is given by $x_\Delta(K)$, i.e., it is the incremental or strain-defined plastic zone. Finally, when the level of externally applied K exceeds that of the last stage of fatigue precracking K_{max} ($K > K_{max}$) the depth of the active plastic zone is given by $x_Y(K)$, i.e., it is the Mises or stress-defined plastic zone.

The described behaviour of the active plastic zone and of the dislocation movement region during rising load HAC affected by fatigue precracking (Fig. 4) provides the required tool for further analysis of the hydrogen-plasticity interactions during the test, as discussed in the following section of the paper.

4. DISCUSSION

To analyse the results of the performed HAC tests on the basis of the described simulation of the crack tip mechanics, it is useful to compare in each experiment the two characteristic distances: (i) the computed depth of the active plastic zone $x_\perp$ and (ii) the measured extension of the hydrogen-assisted damage area ahead of the crack tip (the TTS depth), both at the point of hydrogen assisted fracture of the specimen. To define the former distance, the critical value of the stress intensity factor for HAC, K_{QHAC}, is evaluated from the ratio of the fracture load in hydrogen F_{HAC} to the same in air F_C (Fig. 1) as follows:

$$K_{QHAC} = (F_{HAC}/F_C)\ K_{IC} \qquad (4)$$

Neglecting subcritical crack growth, K_{QHAC} may be considered as an upper bound estimate for the threshold stress intensity factor for HAC.

The definition of K_{QHAC} allows a complete analysis of Fig. 4, where the yielding history is represented for HAC tests after precracking with $K_{max}/K_{IC} = 0.45$ and 0.80. As indicated above, there is a change in the plastic zone from strain-defined (incremental) to stress-defined (von Mises) and this fact produces a kind of sudden increase (an "explosion") of plastic zone size. This sudden increase takes place when the maximum fatigue precracking level is exceeded during the rising-load HAC test, and thus it happens earlier in the lower precracking regimes ($K_{max}/K_{IC} = 0.45$) than in the heavier precracking regimes ($K_{max}/K_{IC} = 0.80$), as represented by the vertical lines in Fig. 4 (dashed for $K_{max}/K_{IC} = 0.45$ and solid for $K_{max}/K_{IC} = 0.80$).

For each experimental fatigue precracking regime, Fig. 5 summarizes the computational results (obtained by the high-resolution finite element analysis described above) in the matter of plasticity spreading. It presents the computed plastic zone sizes during fatigue precracking (forward or monotonic x_Y at the level $K=K_{max}$ and reversed or cyclic x_Δ at the level $K=K_{min} \cong 0$, for a given fatigue precracking intensity K_{max}). The active plastic zone depths $x_\perp$ at fracture in the rising load HAC test are also presented in Fig. 5. These latter regions are defined for corresponding experimental value of $K = K_{QHAC}$ according to the numerical results given by relations (3) and represent the physical domain where dislocation motion *does* take place in the material up to the fracture instant in the HAC test. For the lowest precracking level $K_{max} = 0.28K_{IC}$, the points in Fig. 5 were obtained by extrapolation of the numerical simulation data using relations (3), i.e., supposing a $(K/\sigma_Y)^2$-similitude of the near tip domain.

For lower precracking K_{max}-levels, the corresponding critical values are $K_{QHAC} > K_{max}$, and the active plastic zone at fracture $x_\perp(K_{QHAC})$ corresponds to the monotonic one $x_Y(K_{QHAC})$, whereas for the strongest fatigue precracking regime at $K_{max} = 0.80\ K_{IC}$ the critical value K_{QHAC} does not exceed K_{max} and the advancement of plastic straining is confined to the

smaller cyclic plastic zone, $x_{\perp}(K_{QHAC}) = x_{\Delta}(K_{QHAC})$, cf respective fracture points shown in Fig. 4. Just when the applied K level in a HAC test overpasses the fatigue precracking level ($K>K_{max}$), the active plastic zone changes from strain- to stress-defined, i.e., from cyclic to monotonic (or from reversed to forward), and this change produces a sudden increase of plastic zone size (an "explosion") of the active plastic plastic zone $x_{\perp}$ where plastic flow goes on, i.e., $d\varepsilon^{p}_{eq}/dt > 0$.

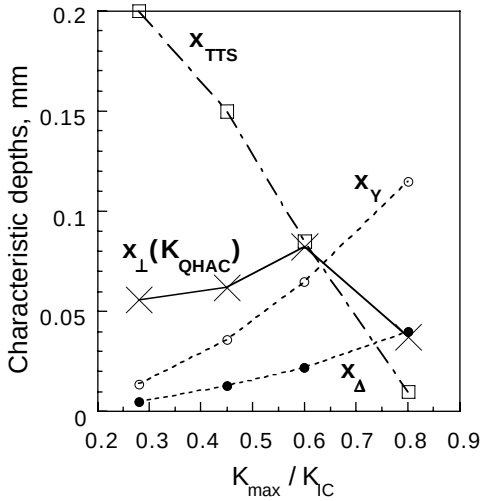

Fig. 5. Comparison of the scales of plasticity spreading and the sizes of the hydrogen-assisted microdamage region (TTS zone) near the crack tip depending on the fatigue precracking regime: dashed lines (with circles) show the sizes of the active cyclic and monotonic plastic zones $x_{\Delta}(K_{max})$ and $x_{Y}(K_{max})$; dashed-doted line (with squares) represents the measured TTS depth x_{TTS}; solid line (with crosses) marks the depth of active plasticity and dislocation movement at the instant of hydrogen assisted fracture in the tests ($K = K_{QHAC}$).

To analyze the coupling between plasticity and hydrogenous effects, Fig. 5 offers the comparison of the calculated extensions $x_{\perp}$ of the active plastic flow (the scales of dislocations mobility) up to the hydrogen assisted fracture event at $K = K_{QHAC}$ and the measured depths x_{TTS} of the hydrogen-assisted microdamage region (TTS) obtained after the HAC tests. With regard to the most forceful fatigue precracking programme with $K_{max}= 0.80K_{IC}$, this K_{max}-level is not surpassed during the HAC experiment because the test terminates just at that level, $K_{QHAC} \approx K_{max}$, only. Obviously, due to measurement errors this latter experimental value of K_{QHAC} may differ from K_{max} within some scatter band. Nevertheless, even if HAC really takes place at K_{QHAC} slightly higher than K_{max}, and so the active plastic zone may have the "burst" size at fracture, $x_{Y}(K_{QHAC})$ but not $x_{\Delta}(K_{QHAC})$ according to expression (3), it must not seriously affect the subsequent deductions from the comparisons of the $x_{\perp}(K_{QHAC})$ and the TTS depth x_{TTS} as far as during the main part of this test the plastic flow is confined to its reduced cyclic dimensions $x_{\Delta}(K)$ out of which insignificant plastic straining can proceed after exceeding K_{max} till soon test termination by HAC.

Fig. 5 demonstrates that plastic zone development does not seem to be a key item in the HAC process, due to the two fundamental experimental facts:

(i) In most experimental fatigue programmes (those with K_{max}/K_{IC} = 0.28, 0.45 and 0.60), the TTS depth is greater than the active plastic zone size associated with the movement of dislocations in the vicinity of the fatigue precrack tip during the HAC test.

(ii) The trends of evolution of the TTS and plastic zone sizes with the level of fatigue preloading K_{max}/K_{IC} is opposite. Whereas the size of the hydrogen-assisted micro-damage region decreases with K_{max}, the plastic zone dimension increases with it.

On the basis of (i), it is possible to say that, in the majority of cases, the hydrogen affected region exceeds the plastic zone, i.e., the only region in which there is dislocation movement, so that hydrogen transport cannot be attributed to dislocation dragging, but only to a random-walk diffusion. It is not, however, conventional diffusion according to classical Fick's laws, but stress-assisted diffusion in which the hydrostatic stress field plays a very important role in accelerating or delaying the diffusion as a function of the sign of its gradient (cf. [3]).

The proposed mechanism of transport by stress-assisted diffusion is consistent with the fundamental experimental fact shown in Fig. 1 of improved HAC behaviour for stronger fatigue precracking regimes. The higher the cyclic load level, the larger the plastic zone and the higher the compressive residual stresses generated near the crack tip after unloading. These compressive stresses are generated by strain compatibility in the plastic near-tip area surrounded by an elastic domain which compresses the former and they produce also negative hydrostatic stress in the vicinity of the crack tip, thus delaying the hydrogen entry and diffusion.

According to (ii) the TTS has no relationship with the plastic zone, and the opposite trend which exhibit these two magnitudes seems to indicate that the role of dislocations in hydrogen transport is reduced by enhancing the trapping of hydrogen instead of transporting it over long penetration distances. This is consistent with experimental observations of the effects of plastic deformation on hydrogen transport in iron, nickel and stainless steel [21] which did not support the assumption that moving dislocations accelerate hydrogen transport because of the two competing effects of enhanced transport and enhanced trapping.

The assumption of increasing trapping of hydrogen as a consequence of fatigue pecracking is consistent with the predamage in the plastic zone created by fatigue (cyclic plastic zone Δx_{PZ}) which delays the hydrogen entry by an increase of the dislocation density an thus of the

number of potential traps for hydrogen. The experimental fact of better HAC performance for increased K_{max} level (Fig. 1) can also be explained by this phenomenon of trapping. The higher the K_{max}-level, the higher the density of traps and the lower the hydrogen entry.

5. CONCLUSIONS

It is shown that cyclic crack-tip plasticity improves the HAC behaviour of the steel, since the failure load in hydrogen is an increasing function of the maximum stress intensity factor during the fatigue precracking.

Fractographic analysis showed that the micro-damage produced by the hydrogen was clearly detectable by scanning electron microscopy, through a specific microscopic topography associated with hydrogen effects: *tearing topography surface* or *TTS*.

High-resolution numerical modelling demonstrated that both the monotonic and the cyclic plastic zone sizes in the fatigue pre-cracking period (numerically computed) stabilise after a few cycles and remain almost constant during fatigue, in spite of the constitutive equation of the material which includes strain hardening.

When cyclic (fatigue) loading is applied during precracking, the active plastic zone changes from the *forward* or *monotonic* one (*stress-defined*) at the maximum load to the *reversed* or *cyclic* one (*strain-defined*) at the minimum load. When the applied level of loading exceeds the historical maximum, a sudden increase ("explosion") of the plastic zone takes place.

In the majority of cases, the hydrogen affected region exceeds the plastic zone, i.e., the only region in which there is dislocation movement, so that hydrogen transport cannot be attributed to dislocation dragging, but only to a random-walk diffusion. It is stress-assisted diffusion, according to which hydrogen is driven by the hydrostatic stress gradient.

The beneficial effect of crack tip plastic straining over the HAC the delay of hydrogen entry caused by compressive residual (hydrostatic) stress after pre-cracking and by enhanced trapping of hydrogen as a consequence of plastic straining, which increases the dislocation density in the vicinity of the crack tip.

Acknowledgments

The financial support (Grant MAT2002-01831) of this work by the Spanish Ministry of Science and Technology (MCYT) and FEDER is gratefully acknowledged. In addition, the authors wish to express their gratitude to EMESA TREFILERIA S.A. (La Coruña, Spain) for providing the steel used in the experimental programme.

REFERENCES

[1] A.R. Troiano, *Trans. ASM* **52** (1960) 54.

[2] H.P. Van Leeuwen, *Engng. Fracture Mech.* **6** (1974) 141.

[3] J. Toribio and V. Kharin, *Fat. Fract. Engng. Mater. Struct.* **20** (1997) 729.

[4] J.K. Tien, A.W. Thompson, I.M. Bernstein and R.J. Richards, *Metall. Trans*. **7A** (1976) 821.

[5] H.H. Johnson and J.P. Hirth, *Metall. Trans.* **7A** (1976) 1543.

[6] S.V. Nair, R.R. Jensen and J.K. Tien, *Metall. Trans.* **14A** (1983) 385.

[7] J. Toribio, *J. Mater. Sci.* **28** (1993) 2289.

[8] J. Toribio, *J. Mater. Sci. Lett.* **11** (1992) 1151.

[9] J. Toribio, *Mater. Sci. Engng*. **A219** (1996) 180.

[10] J. Toribio and A.M. Lancha, *J. Mater. Sci. Lett.* **11** (1992) 1085.

[11] J. Toribio and A.M. Lancha, *J. Mater. Sci. Lett.* **14** (1995) 1204.

[12] J. Toribio and A.M. Lancha, *J. Mater. Sci.* **31** (1996) 6015.

[13] R.N. Parkins, M. Elices, V. Sánchez-Gálvez and L. Caballero, *Corros. Sci.* **22** (1982) 379.

[14] A.W. Thompson and J.C. Chesnutt, *Metall. Trans.* **10A** (1979) 1193.

[15] J.E. Costa and A.W. Thompson, *Metall. Trans.* **13A** (1982) 1315.

[16] J. Toribio, A.M. Lancha and M. Elices, *Scripta Metall. Mater.* **25** (1991) 2239.

[17] J. Toribio, A.M. Lancha and M. Elices, *Metall. Trans.* **23A** (1992) 1573.

[18] J. Toribio, *Metall. Mater. Trans*. **28A** (1997) 191.

[19] K.J. Handerhan and W.M. Garrison: *Acta Metall. Mater.* **40** (1992) 1337.

[20] MARC User Information, Marc Analysis Research Corp., Palo Alto, 1994.

[21] T. Zakroczymski, *Corrosion* **41** (1985) 485.